European Journal of Soil Science

European Journal of Soil Science, February 2010, **61**, 108–119 doi: 10.1111/j.1365-2389.2009.01207.x

Diffusion of strongly sorbed solutes in soil: a dual-porosity model allowing for slow access to sorption sites and time-dependent sorption reactions

M. Ptashnyk[a], T. Roose[a] & G. J. D. Kirk[b]

[a]*Centre for Mathematical Biology, Mathematical Institute, University of Oxford, 24-29 St Giles', Oxford OX1 3LB, UK, and* [b]*National Soil Resources Institute, Natural Resources Department, Cranfield University, Cranfield MK43 0AL, UK*

Summary

We use homogenization techniques to derive a dual (or double) porosity model of solute diffusion and reaction in soil, allowing for slow access to sorption sites within micro-aggregates and time-dependent sorption reactions. We give a means for determining the conditions in which micro-scale concentration gradients affect macro-scale gradients and fluxes. We present equations for a unit volume of soil represented as a series of uniformly-spaced, porous spherical particles, containing and surrounded by solution through which solutes diffuse. The methods we use can, in principle, be applied to more complex geometries. We compare the model's predictions with those of the equivalent single porosity model for commonly used boundary conditions. We show that failure to allow for slow access to reaction sites can lead to seriously erroneous results. Slow access has the effect of decreasing the sorption of solute into soil from a source or desorption from soil to a sink. As a result of slow access, the diffusion coefficients of strongly-sorbed solutes measured at the macro-scale will be time-dependent and will depend on the method of measurement. We also show that slow access is more often likely to limit macro-scale diffusion than rates of slow chemical reactions *per se*. In principle, the unimportance of slow reactions except at periods longer than several weeks of diffusion simplifies modelling because, if slow access is correctly allowed for, sorption can be described with equilibrium relations with an understanding of speciation and rapid sorption-desorption reactions.

Introduction

This paper is about the prediction of diffusion in soil when local equilibration between the diffusate and soil particles is slow compared with diffusion through the soil bulk. The processes resulting in slow equilibration are likely to be most important for strongly sorbed solutes, such as phosphate and contaminants including many heavy metals and radionuclides. The potentially rate-limiting steps include access to sorption sites within particles as well as slow sorption reactions (Tinker & Nye, 2000; Barrow, 2008; Sposito, 2008). Which of these is dominant has implications for modelling and measurement. However, few models of diffusion in soil deal with these processes explicitly, and most kinetic studies are made in shaken suspensions in which access to sorption sites may be increased by disaggregation and convection. Nonetheless, failure to allow correctly for slow access and true reaction kinetics in models can produce misleading results, as we will show.

Modelling such systems is complicated. Where solute concentration gradients at the macro-scale, for example the scale of a plant root or an experimental soil column, depend on processes controlled by gradients at much finer scales such as a pore within a soil particle, it is difficult to solve and link together the relevant equations across scales. We know of only two examples where this has been attempted. Staunton & Nye (1989) developed a model of diffusion along a soil column in which local equilibration depended on diffusion into spherical aggregates. With the numerical methods that they used it was necessary to decouple the inter- and intra-aggregate pathways and solve the resulting equations separately. Only a simple equilibrium treatment of sorption reactions was possible, and diffusion within the aggregates was only radial and made no contribution to the longitudinal flux. Nye & Staunton (1994) avoided these problems and included time-dependent reactions by representing unit volume of soil as a hollow cylinder with its axis in the direction of the longitudinal flux, and with parallel inter- and intra-aggregate pathways

Correspondence: Guy Kirk. E-mail: g.kirk@cranfield.ac.uk.

Received 30 June 2008, revised version accepted 8 October 2009

© 2009 The Authors
Journal compilation © 2009 British Society of Soil Science

represented by the central and outer cores of the cylinder. The resulting equations could be solved together using standard methods. However, this geometry gives a poor representation of a real soil and the physical basis of a continuous intra-aggregate pathway is weak. An alternative approach, with which more realistic geometries and reaction terms can be tackled, is provided by the method of homogenization (Bourgeat *et al*., 1996; Hornung, 1997; Pavliotis & Stuart, 2008). This gives a means of transforming equations at different scales into a single, tractable set of equations. Thereby it is possible to define equations at the macro-scale that implicitly allow for processes and geometries at the micro-scale.

In this paper we use the method of homogenization to develop a dual-porosity model of diffusion and reaction in soil, with which to assess the importance of slow access to sorption sites versus rates of sorption reactions *per se*. We treat the soil as a series of porous spherical particles, *pace* Staunton & Nye (1989). We use multiple space-scale analysis to derive equations at the macroscopic, whole-soil scale, and base the coupling between the microscopic, sub-particle scale and the macroscopic scale on the microscopic interaction between the intra- and extra-particle spaces. Multiple space-scale analysis of this sort is a generalization of the more well-known multiple timescale approach (Kevorkian & Cole, 1996; Bender & Orszag, 1999). We derive models for movement at the macro-scale for different parameter regimes, and solve the resulting equations using standard numerical packages. To avoid undue geometrical complexity we consider a system of uniformly spaced spherical particles. This corresponds approximately to experiments in which soil has been sieved to give roughly uniform micro-aggregates, and then re-packed to a uniform bulk density. The approach is applicable to more complex geometries.

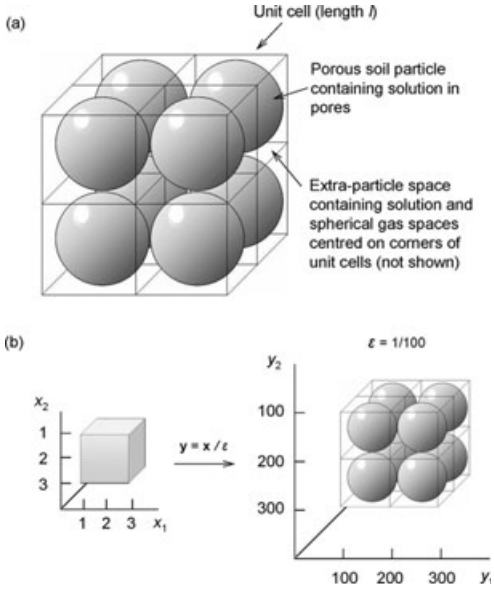

Figure 1 The geometry of the model. (a) The upper figure shows eight unit cells, each containing one porous soil particle (shaded) and its associated extra-particle liquid and gas (not differentiated in the figure). The particles are in a loose cubic arrangement with the edges of neighbouring particles separated by a thin liquid layer thickness δ. (b) The lower figure illustrates homogenization across scales. The left-hand graph is in coarse **x** coordinates and shows the macrostructure of the system; the right-hand graph is in finer **y** coordinates and reveals the microstructure. The scaling parameter ε equals 1/100: a 100-fold magnification of the macroscopic scale is necessary to reveal the microstructure.

Theory

The nomenclature is explained in Table 1.

Geometry of the model

We consider a column of moist soil of uniform bulk density. We represent unit volume of soil as a series of uniformly-spaced porous spherical particles containing solution within the pores and surrounded by further solution and gas spaces (Figure 1a). The radius of the soil particles is determined by the sieve mesh of the soil, and their porosity is determined by the soil bulk density and solid density. Solute applied at or removed from one end of the soil column diffuses longitudinally in the extra-particle pores, and both longitudinally and radially in the intra-particle pores, and it is simultaneously sorbed by soil surfaces inside and outside the particles in time-dependent reactions. We consider two types of reactions: one fast and one slow relative to diffusion through the soil. We discuss the empirical basis of the fast and slow reactions later under 'Parameter values'.

The following assumptions are implied by this geometry: (i) the soil micro-aggregates can be represented as porous spherical particles, (ii) the particles are surrounded by macro-pores that are interconnected, (iii) a continuous film of liquid is in contact with and connects the particles, and (iv) the soil air tends to occupy the centre of the pores between particles.

We therefore have a composite material with microscopic properties that change periodically and rapidly compared with the macroscopic scale. We define macroscopic space variable **x** and microscopic space variable **y** (Figure 1b). The characteristic macroscopic length-scale is the length b of the soil column; the characteristic microscopic length-scale is the length l of the unit cell containing a soil particle and its associated extra-particle liquid and gas. If the ratio of the two length scales is small, i.e. scaling parameter $\varepsilon = l/b \ll 1$, it is possible to use homogenization theory to find effective macroscopic properties. Homogenization allows us to develop equations allowing for the influence of both spatial coordinates: the **y** coordinates reflecting the microscopic properties of the system, and the coarser **x** coordianates reflecting the macroscopic properties. Homogenization theory considers that **x** and **y** can be treated independently if ε is sufficiently small.

We first define dimensional equations for the model. We then make these dimensionless by using the scale of the microscopic

© 2009 The Authors
Journal compilation © 2009 British Society of Soil Science,

Table 1 Nomenclature

Symbol	Meaning	Units
$\mathbf{x}$	Space variable for macroscopic scale (i.e. scale of a soil column) (Cartesian coordinates x_1, x_2, x_3)	cm
$\mathbf{y}$	Space variable for microscopic scale (i.e. scale of a single soil particle) (Cartesian coordinates y_1, y_2, y_3)	cm
a	Radius of soil particle	cm
b	Length of soil column	cm
c	Radius of soil column	cm
l	Length of unit cell containing a soil particle and its associated extra-particle liquid and gas	cm
ε	Scaling parameter relating micro- and macro-scopic length-scales, $\varepsilon = l/b$	–
ν	Vector normal to particle or gas-space surface (positive inwards)	–
t	Time	s
C	Concentration of solute per unit whole soil volume	μmol cm^{-3} (soil)
L_e, L_i	Concentration of solute in extra-, intra-particle liquid	μmol cm^{-3} (liquid)
S_e, S_i	Concentration of solute on extra-, intra-particle surfaces per unit solid mass (subscripted 1 or 2 for rapidly- and slowly-reacting solute, respectively)	μmol g^{-1} (solid)
k_{Fe}, k_{Be}	Rate constant for forward, backward sorption reaction on extra-particle surfaces (subscripted as S)	s^{-1}
k_{Fi}, k_{Bi}	Rate constant for forward, backward sorption reaction on intra-particle surfaces (subscripted as S)	s^{-1}
α	Coefficient in equilibrium sorption equation (subscripted as S)	–
β	Coefficient in equilibrium sorption equation (subscripted as S)	μmol$^{1-\alpha}$ cm$^{3\alpha}$ g^{-1}
θ	Water content of whole soil per unit whole soil volume	cm^3 cm^{-3} (soil)
θ_e	Water content of extra-particle space per unit extra-particle space volume	cm^3 cm^{-3} (liquid)
θ_i	Water content of particle per unit particle volume	cm^3 cm^{-3} (particle)
θ_e', θ_i'	θ_e, θ_i per unit whole soil volume	cm^3 cm^{-3} (soil)
ρ	Soil solid mass per unit whole soil volume	g cm^{-3} (soil)
ρ_i	Soil solid mass per unit particle volume	g cm^{-3} (particle)
ρ_s	Soil solid mass per unit solid volume	g cm^{-3} (solid)
ϕ_e', ϕ_i'	Porosity of extra- intra-particle space	cm^3 cm^{-3} (soil)
σ_e	Soil mass per unit external surface area of particle	g cm^{-2} (ext. particle)
σ_i	Soil mass per unit internal surface area of particle	g cm^{-2} (int. particle)
D_i	Diffusion coefficient of solute in intra-particle pores $= \theta_i f_i D_l$	cm^2 s^{-1}
D_l	Diffusion coefficient of solute in free solution	cm^2 s^{-1}
f_e,f_i	Impedance factor for diffusion in inter-, intra-particle pores	–
∇	Partial differential operator in 3-D space ($= (\partial/\partial x_1, \partial/\partial x_2, \partial/\partial x_3)$)	–

space, re-scale to obtain equations on the scale of the soil bulk, and then apply homogenization theory to obtain the the macroscopic equations.

Dimensional model

The continuity equation for diffusion in the liquid around a particle is (L_e is the concentration in the extra-particle liquid):

$$\frac{\partial L_e}{\partial t} = \nabla\cdot(D_l \nabla L_e), \tag{1}$$

and the continuity equation for diffusion and reaction in the particle is (L_i is the concentration in the intra-particle liquid)

$$\frac{\partial(\theta_i L_i)}{\partial t} = \nabla\cdot(D_i \nabla L_i) - \frac{\partial(\rho_i S_{i1})}{\partial t} - \frac{\partial(\rho_i S_{i2})}{\partial t}, \tag{2}$$

where the last two terms allow for the fast and slow sorption reactions on surfaces inside the particle. These equations need to be coupled *via* boundary conditions at the particle surface. The boundary conditions showing the solute flux and concentration continuity at the particle surface, and allowing for the fast and slow sorption reactions on the external particle surface, are:

$$D_l \nabla L_e\cdot\nu = D_i \nabla L_i\cdot\nu - \frac{\partial(\sigma_e S_{e1})}{\partial t} - \frac{\partial(\sigma_e S_{e2})}{\partial t}, \tag{3}$$

and

$$L_e = L_i. \tag{4}$$

On the surfaces of the extra-particle gas spaces we apply a zero flux boundary condition:

$$D_l \nabla L_e\cdot\nu = 0. \tag{5}$$

As stated previously, L_e and L_i are the solute concentrations in the extra- and intra-particle liquid, and S_{e1}, S_{e2}, S_{i1} and S_{i2} are the concentrations of rapidly- and slowly-reacting solute on external and internal particle surfaces, respectively. The rates of reaction are functions of L and S as described later. The term ν is the vector normal to the soil particle or air particle surface.

© 2009 The Authors
Journal compilation © 2009 British Society of Soil Science,

Non-dimensional model

We now make Equations (1)–(5) dimensionless to facilitate the multi-scale analysis. In order to couple processes at the micro- and macro-scales, we scale space by using the microscopic length-scale of the unit cell containing a single soil particle, and time by using the macroscopic diffusional timescale based on the length of a soil column, that is to the time-scale of experimental interest. Hence, using asterisks to indicate dimensionless variables,

$$\mathbf{y} = (ly_1^*, ly_2^*, ly_3^*), \quad \text{and}$$
$$t = (b^2/D_l)t^*.$$

Also we scale concentration with unit concentration, and, because $L_e = L_i$ at the particle surface, we scale L_e and L_i the same. Hence:

$$L_e = L \times L_e^* \quad \text{and}$$
$$L_i = L \times L_i^*,$$

where L is the characteristic solute concentration scale, which we take to be $\mathrm{L} = 1$ μM. The scalings for the amounts of sorbed solutes are:

$$S_e = (l/\sigma_e)S_e^* \quad \text{and}$$
$$S_i = (1/\rho_i)S_i^*,$$

where ρ_i is the solid mass per unit particle volume and σ_e is the soil mass per unit external particle surface area.

With these scales the dimensionless forms of Equations (1)–(5) in **y** coordinates (the microscale coordinates), dropping the asterisks, are:

$$\frac{\partial L_e}{\partial t} = \frac{1}{\varepsilon^2}\nabla_y^2 L_e \quad \text{in extra-particle space,} \tag{1a}$$

$$\frac{\partial(\theta_i L_i)}{\partial t} = \frac{D_i}{D_l\varepsilon^2}\nabla_y^2 L_i - \frac{\partial S_{i1}}{\partial t} - \frac{\partial S_{i2}}{\partial t} \quad \text{in particle,} \tag{2a}$$

$$\nabla_y L_e \cdot \nu = \frac{D_i}{D_l}\nabla_y L_i \cdot \nu - \varepsilon^2\frac{\partial S_{e1}}{\partial t} - \varepsilon^2\frac{\partial S_{e2}}{\partial t} \quad \text{on particle surface,} \tag{3a}$$

$$L_e = L_i \quad \text{on particle surface,} \tag{4a}$$

$$\nabla_y L_e \cdot \nu = 0 \quad \text{on gas-space surfaces.} \tag{5a}$$

Homogenized model

For our standard parameter values (see later), the ratio of the diffusion coefficients inside and outside the particle $D_i/D_l \approx \varepsilon^2$. This means the term $D_i/(D_l\varepsilon^2)$, which multiplies the space derivative in Equation (2a), is of the order of one, and the spatial and temporal solute dynamics inside the particle are therefore properly coupled to the dynamics outside the particle. If this was not so, the effective macro-scale model would not reflect the micro-scale processes, in other words, the within-particle dynamics would not constrain solute movement on the macro-scale. Having set the conditions for coupling the micro- and macro-scales, we can re-scale Equations (1a)–(5a) from the single particle to the whole soil using $\mathbf{x} = \varepsilon\mathbf{y}$, and obtain the homogenized macro-scale model. We summarize the derivation of the model for $D_i/D_l \approx \varepsilon^2$ in the Appendix, and also give the models for $D_i/D_l \approx \varepsilon$ and ε^3. The model for $D_i/D_l \approx \varepsilon^2$ is as follows.

We denote the macroscopic space domain bounded by the external surfaces of the soil column as Ω, the microscopic space domain within soil particles as Y, and the domain of soil particle surfaces as Γ. The effective macro-scale model for $D_i/D_l \approx \varepsilon^2$ is then:

$$\frac{\partial(\theta_e' L_e)}{\partial t} = \nabla_x \cdot (\theta_e' f_e \nabla_x L_e) + \frac{1}{|Z|}\int_\Gamma \left(\hat{D}\nabla_y L_i \cdot \nu - \frac{\partial S_{e1}}{\partial t} - \frac{\partial S_{e2}}{\partial t}\right) d\gamma \quad \text{in } \Omega, \tag{6}$$

$$L_e = L_i \quad \text{on} \quad \Gamma \times \Omega, \tag{7}$$

$$\frac{\partial(\theta_i L_i)}{\partial t} = \hat{D}\nabla_y^2 L_i - \frac{\partial S_{i1}}{\partial t} - \frac{\partial S_{i2}}{\partial t} \quad \text{in } \mathrm{Y} \times \Omega, \tag{8}$$

where f_e is the impedance factor for the extra-particle space ($= A_\mathrm{hom}/\theta_e'$ where A_hom is effective diffusion matrix derived in the Appendix), $|Z|$ is the volume of a single soil particle in **y** coordinates, $\hat{D} = D_i/(D_l\varepsilon^2)$ is the dimensionless diffusion coefficient within the particle, and the term under the integral in Equation (6) is integrated over the particle surface Γ.

The macro-scale boundary condition at $x_1 = 0$ (surface denoted Γ_D) is determined by the means of application or removal of the solute, and the condition at all other external boundaries (surfaces denoted Γ_N) is that there is no transfer of solute, i.e.:

$$L_e = L_{eD} \quad \text{on} \quad \Gamma_D. \tag{9}$$

$$\nabla_x L_e \cdot \nu = 0 \quad \text{on} \quad \Gamma_N. \tag{10}$$

Equations (6)–(10) constitute a dual porosity model that is valid when the ratio of intra- and extra-particle diffusion coefficients $D_i/D_l \approx \varepsilon^2 = (l/b)^2$. We choose as standard for the simulations below the length of the single particle domain $l = 0.02$ cm and the length of the soil column $b = 2$ cm; these are appropriate for an experiment (see Staunton & Nye, 1989) in which soil has been sieved to 0.02 cm and repacked in a column 2-cm long. Hence $\varepsilon = 1/100$, and $D_i/D_l \approx 2 \times 10^{-4}$ (see later) $\approx \varepsilon^2$. The model should be valid for D_i/D_l values that are 10-fold greater or smaller than this with $\varepsilon \approx 1/100$.

For $D_i/D_l \approx \varepsilon$ (e.g. $l = 0.02$ cm, $b = 100$ cm and D_i/D_l as later), the effective macro-scale model is Equation (A10) in the Appendix. In this case, diffusion within the particle is fast relative to that outside and thus the concentration profile within the particle is flat. However, the rate of reaction inside the particle is important on the macroscopic scale and so we

© 2009 The Authors

have a standard, impeded diffusion model with source/sink terms that allow for sorption on surfaces inside and outside particles. For $D_i/D_l \approx \varepsilon^3$ (e.g. $l = 0.02$ cm, $b = 0.4$ cm and D_i/D_l as below), the effective macro-scale model is Equation (A11) in the Appendix. The diffusion into and inside the particle is now too slow to influence macro-scale processes and the equations for the concentrations inside the particle are not coupled with the macroscopic equations.

The remainder of the paper is concerned only with the dual-porosity model given by Equations (6)–(10).

Kinetics of the sorption reactions

We represent the sorption-desorption reactions on internal and external particle surfaces with the following Freundlich-type equations:

$$\frac{\partial(\rho_i S_i)}{\partial t} = k_{Fi}(\theta_i L_i)^{\alpha} - k_{Bi}\rho_i S_i, \tag{11}$$

and

$$\frac{\partial(\sigma_e S_e/l)}{\partial t} = k_{Fe}(\theta_e^{'} L_e)^{\alpha} - k_{Be}\sigma_e S_e/l, \tag{12}$$

where k_F and k_B are forward and backward rate constants (omitting subscripts 1 and 2 for fast and slow reactions) and α is a coefficient with value between 0 and 1 ($\alpha = 1$ being for linear sorption). The non-dimensional forms of Equations (11) and (12) are (dropping asterisks):

$$\frac{\partial S_i}{\partial t} = k_{Fi} L_i^{\alpha} - k_{Bi} S_i, \tag{11a}$$

and

$$\frac{\partial S_e}{\partial t} = k_{Fe} L_e^{\alpha} - k_{Be} S_e. \tag{12a}$$

Simplification of the model

We simplify the homogenized model by considering conditions for which the fast reactions are effectively instantaneous compared with diffusion through the soil solution, i.e. $k_{B1}b^2/D_l \gg 1$. Also, because the particles are separated by extra-particle solution and diffusion in the extra-particle solution is fast, there are no longitudinal gradients within the particles and diffusion in them is only radial. Therefore we can reduce the general model to a set of one-dimensional equations for L_e and L_i coupled *via* the boundary condition on the particle surface. We consider a soil column of dimensionless length $x_1 = 1$ and particles of radius $r = a$ where r is the radial coordinate within a particle (r varies from 0 to a). Thereby we obtain:

$$\left(\theta_e^{'} + 4\pi a^2 l \frac{k_{Fe1}}{k_{Be1}} \theta_e^{'\alpha} \alpha L_e^{\alpha-1}\right) \frac{\partial L_e}{\partial t} = \frac{\partial}{\partial x_1}\left(\theta_e^{'} f_e \frac{\partial L_e}{\partial x_1}\right) - 4\pi a^2 l \left[l \frac{\partial(\hat{D} L_i)}{\partial r}|_{r=a} + (k_{Fe2} L_e^{\alpha} - k_{Be2} S_{e2}) \right] \quad \text{in } (0 \le x_1 \le 1), \tag{13}$$

$$L_e = L_i \quad \text{on } (r = \text{a}) \times (0 \le x_1 \le 1), \tag{14}$$

$$\left(\theta_i + \frac{k_{Fi1}}{k_{Bi1}} \theta_i^{\alpha} \alpha L_i^{\alpha-1}\right) \frac{\partial L_i}{\partial t} = \frac{1}{r^2}\frac{\partial}{\partial r}\left(r^2 l^2 \frac{\partial(\hat{D} L_i)}{\partial r}\right) - (k_{Fi2} L_i^{\alpha} - k_{Bi2} S_{i2}) \quad \text{in } (0 \le r \le a) \times (0 \le x_1 \le 1). \tag{15}$$

Solution of the equations

We solved Equations (13)–(15) numerically using finite-difference approximations for the space derivatives and Matlab ODE solver ode15s to solve the resulting ordinary differential equations. In the results presented below, we give calculated concentration-distance profiles of L_e and C along a soil column subject to specified boundary conditions, where C is the total solute concentration at a particular distance, equal to the sum of concentrations in the solid and solution taking account of the distributions inside the particle.

Results and discussion

Parameter values

The standard parameter values for the simulations below are derived as follows. The set of primary values is given in Table 2.

Geometry. The relations between the soil bulk density, water content and gas content are constrained by the model geometry. We have for the total soil porosity:

$$\phi = \phi_e^{'} + \phi_i^{'} = 1 - \rho/\rho_s, \tag{16}$$

Table 2 Parameter values for the simulations in Figures 2–6

Parameter	Value	Parameter	Value
a	9.98×10^{-3} cm	α	1
b	2 cm	β_1	500 cm^3 g^{-1}
l	0.02 cm	β_2	1500 cm^3 g^{-1}
ρ	1.1 g cm^{-3} (soil)	k_{F2}	10^{-4} s^{-1}
ρ_s	2.65 g cm^{-3} (solid)	D_l	9×10^{-6} cm^2 s^{-1}
$\phi_e^{'}$	0.48 cm^3 cm^{-3} (soil)	f_e	0.628
σ_i	5×10^{-4} g cm^{-2} (int. particle)	f_i	0.001

All other parameters are derived from these parameters, as described in the text.

© 2009 The Authors
Journal compilation © 2009 British Society of Soil Science,

where ϕ_e' and ϕ_i' are the porosities of the extra- and intra-particle spaces, respectively, and ρ_s is the density of the soil solid. The upper limit on ϕ_e' as the thickness of the liquid layer around a particle (δ in Fig. 1) $\rightarrow 0$ is $(l^3 - 4/3\pi a^3)/l^3 = 1 - 4/3\pi(0.5)^3 = 0.476$. We choose $\phi_e' = 0.48$, which means that $a = 9.98 \times 10^{-3}$ cm. The upper limit on the gas content, and hence the lower limit on the water content, is set by the maximum size of spherical gas spaces that can be accommodated in the corners of the unit cell. From the relevant triangles in the unit cell, this gives for the maximum radius of the gas spaces:

$$a_g = \sqrt{3/4 \times l^2} - l/2. \tag{17}$$

Hence the volume of the gas spaces per unit whole soil volume is

$$\phi_e' - \theta_e' = 4/3\pi a_g^3/l^3. \tag{18}$$

Thus for $l = 0.02$ cm and $\phi_e' = 0.48, \theta_e' = 0.274$. Therefore, for $\rho = 1.1$ g cm^{-3} and $\rho_s = 2.65$ g cm^{-3}, $\phi_i' = 1 - \rho/\rho_s - \phi_e' = 0.105$, and because the intra-particle space is assumed to be water-saturated, $\theta_i' = \phi_i' = 0.105$ and $\theta = \theta_e' + \theta_i' = 0.379$: $\theta_e = \theta_e'/\phi_e' = 0.571$ and $\theta_i = \theta_i'/(1 - \phi_e') = 0.202$.

The specific surface area of the external particle surface is $SSA_e = 4\pi a^2/(l^3\rho)$, that is $\sigma_e = 1/SSA_e = 7.03 \times 10^{-3}$ g cm^{-2}. The specific surface area of the internal particle surface depends on how the total internal porosity is distributed amongst pores of different sizes and is a function of the composition of the particle as well as its total porosity. Typical values are $SSA_i = 500$ to 15 000 cm^2 g^{-1}, that is $\sigma_i = 2 \times 10^{-3}$ to 6.7×10^{-5} g cm^{-2}.

Diffusion. With spherical gas spaces in the corners of the unit cell, the impedance factor for the extra-particle space, $f_e = 0.628$ (see Appendix) (note that other gas space geometries can be specified, resulting in different values of f_e; alternatively, an experimentally measured f_e can be used). We take as standard $f_i = 0.001$, which is the value used by Nye & Staunton (1994) to fit their model to experimental data for P diffusion. The diffusion coefficient in the intra-particle space is $D_i = \theta_i f_i D_l$. With $f_i = 0.001$, $\theta_i = 0.202$ and $D_l = 9 \times 10^{-6}$ cm^2 s^{-1} (the value for $H_2PO_4^-$), $D_i = 1.82 \times 10^{-9}$ cm^2 s^{-1}. For the simulations for non-sorbed solutes in Figure 2, we use $D_l = 2 \times 10^{-5}$ cm^2 s^{-1} (the value for Cl^-).

Sorption. In the simplified model we represent sorption as an instantaneous reaction followed by a much slower one. Measurements of sorption kinetics in shaken soil suspensions often indicate several relatively fast reactions lasting minutes or hours followed by much slower reactions continuing for days or weeks (Sposito, 2008). Simple sorption-desorption reactions should be complete within a matter of minutes, and be effectively instantaneous compared with diffusion. The much slower reactions may involve specific sorption, precipitation, solid-state diffusion, or other processes (Sposito, 2008). However, the slower 'fast' reactions observed in shaken suspensions can be accounted for by slow diffusive penetration of soil particles as we now show (after Nye & Staunton, 1994). The half-time for diffusion into a spherical particle of radius a maintained at a constant external concentration is $\sqrt{Dt/a^2} = 0.18$ (Crank, 1975, Fig. 6.7), where D is the effective intra-particle diffusion coefficient with instantaneous sorption, given by $D = D_l\theta_i f_i/(\rho_i\beta_{i1})$ where β_{i1} is the solid : solution partition coefficient. With our standard values of a, D_l, θ_i, f_i and ρ_i and a typical value of $\beta_{i1} = 500$, this gives $t_{1/2} = 2.2 \times 10^6$ s $\equiv 25$ d. If the slow penetration into the particle is represented as a first order reaction, given by (compare Equation (11)) $\partial(\rho_i S)/\partial t = k_F\theta_i L_e - k_B\rho_i S$, where k_F and k_B are forward and backward rate constants, then from the integral of this equation, remembering L_e is constant, the half-time of the reaction is $t_{1/2} = \ln 2/k_B$. Thus the half-time of 2.2×10^6 s for diffusive penetration calculated above would correspond to $k_B = 3.15 \times 10^{-7}$ s^{-1}. The corresponding value of k_F in a shaken suspension experiment would be $k_B \times \beta_{i1} = 1.6 \times 10^{-4}$ s^{-1} or a half-time for sorption of 1.3 hours This is comparable with the values observed for 'fast' reactions in shaken suspensions, and an order of magnitude faster than the 'slow' reactions. We conclude that our representation of sorption as an instantaneous reaction and a slow reaction is realistic.

We relate the parameters in Equations (11) and (12) for sorption on internal and external surfaces to the corresponding, measurable parameters for the whole soil as follows. We have for the whole soil (dropping the subscripts 1 and 2 for fast and slow reactions):

$$\frac{\partial(\rho S)}{\partial t} = k_F(\theta L)^\alpha - k_B\rho S. \tag{19}$$

At equilibrium, $\partial S/\partial t = 0$ and Equation (19) gives a Freundlich equation:

$$S = \beta L^\alpha \quad \text{where} \quad \beta = k_F\theta^\alpha/(k_B\rho). \tag{20}$$

We assume that the density of sorption sites on external and internal surfaces is the same and that $\sigma_i S_i = \sigma_e S_e$. Also $k_{Bi} = k_{Be} = k_B$. Thereby we obtain for the reactions on internal surfaces:

$$k_{Fi} = k_F \frac{(\theta/\theta_i)^\alpha}{(1 + \sigma_i/\sigma_e)} \frac{\rho_i}{\rho}, \tag{21}$$

and

$$\beta_i = k_{Fi}\theta_i'^\alpha/(k_{Bi}\rho_i) = \beta/(1 + \sigma_i/\sigma_e), \tag{22}$$

and for the reactions on external surfaces:

$$k_{Fe} = k_F \frac{(\theta/\theta_e')^\alpha}{(1 + \sigma_e/\sigma_i)} \frac{\sigma_e}{l\rho}, \tag{23}$$

and

$$\beta_e = k_{Fe}\theta_e'^\alpha/(k_{Be}\sigma_e/l) = \beta/(1 + \sigma_e/\sigma_i). \tag{24}$$

© 2009 The Authors

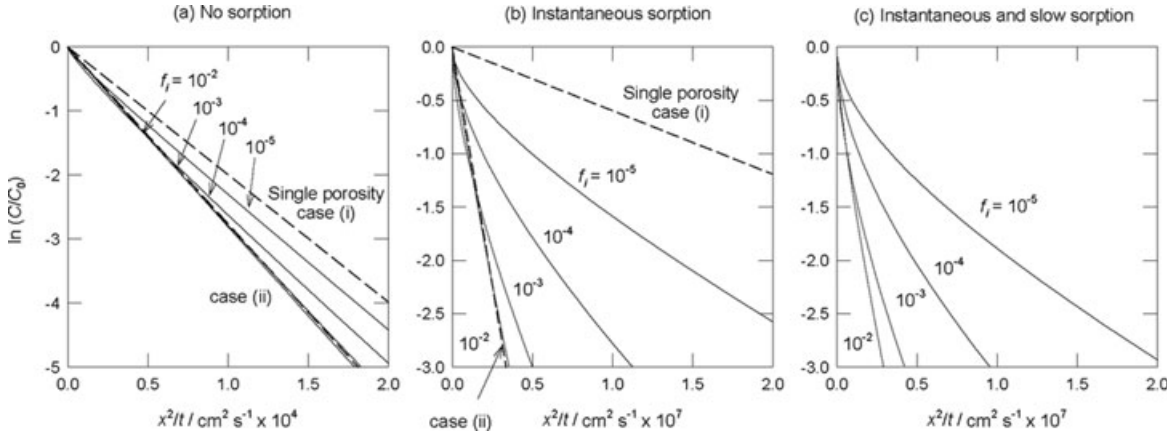

Figure 2 Plots of In C/C_0 against x^2/t for a solute initially deposited at the surface of a soil column with (a) no solute sorption, (b) instantaneous sorption and (c) instantaneous sorption plus continuing slow sorption. Full lines are the predictions of the dual porosity model with different values of f_i; dotted lines are for the single porosity model with either no (case i) or instantaneous (case ii) intra-particle equilibration (D given by Equations (27) and (28), respectively). Run times 10^4 s for (a) and 5×10^6 s for (b) and (c). Note the larger scale of the x-axis of (a).

For simplicity we choose linear sorption with $\alpha = 1$, which is realistic for isotopic exchange or a narrow concentration range. We take as standard the following values from Nye & Staunton (1994) for sorption of P on a sandy loam soil: $\beta_1 = 500$, $\beta_2 = 1500$ and $k_{F2} = 10^{-4}$ s^{-1}.

Applications

We now illustrate the applications of the model for analysing experiments on diffusion and reaction in soil. We compare its predictions with those of the simple single-porosity model in which local equilibration is instantaneous and only diffusion in the inter-particle pores contributes to diffusion down the soil column. In particular, we study the case of a pulse application of solute at the surface of a soil column, for which the single porosity model has a simple linear form.

Pinner & Nye (1982) showed that, for a pulse application, if local equilibration is instantaneous a plot of log C against x^2/t (where C is concentration and x is distance normal to the application surface) should be linear, but if equilibration is slow the plot should be curved. This has been exploited by Nye and colleagues to measure the self-diffusion and surface interactions of a wide range of solutes in soil. In self-diffusion there is no net exchange of sorbed species and so the sorption reactions are necessarily linear. They found that results for the self-diffusion of non-adsorbed Cl^- ions gave linear plots (Pinner & Nye, 1982; So & Nye, 1989; Kirk *et al*., 2003), and results for the self-diffusion of the exchangeable cations Na^+, Ca^{2+}, Rb^+ and Cs^+ also gave approximately linear plots (references in Nye & Staunton, 1994). However, plots for the self-diffusion of phosphate were curved (Staunton & Nye, 1989), indicating non-instantaneous equilibration.

We discuss Nye and colleagues' findings in the light of the dual-porosity results for a pulse boundary condition. We also give results for the more practically important boundary conditions of a constant concentration of solute at the soil surface (for example for diffusion from a band of fertilizer) and a zero concentration at the surface (for example for diffusion to a root mat or to a DGT device: Ernstberger *et al*., 2002).

Instantaneous source at soil surface. The single porosity model in planar geometry when local equilibration is instantaneous is:

$$\frac{\partial C}{\partial t} = \frac{\partial}{\partial x}\left(D_l \theta_e' f_e \frac{\partial L_e}{\partial x}\right) = \frac{\partial}{\partial x}\left(D_l \theta_e' f_e \frac{dL_e}{dC}\frac{\partial C}{\partial x}\right) = \frac{\partial}{\partial x}\left(D\frac{\partial C}{\partial x}\right), \qquad (25)$$

where C is the total concentration of solute in the soil, D is the effective soil diffusion coefficient and x is the distance along the soil column ($\equiv x_1$ in the dual-porosity model). For a pulse application of solute at $x = 0$, zero initial concentration in the soil column, and instantaneous local equilibration with linear or no sorption, the solution of Equation (25) is (Pinner & Nye, 1982, after Crank, 1975, Equation 2.6):

$$\frac{C}{C_0} = \exp\left(-\frac{x^2}{4Dt}\right), \qquad (26)$$

where C_0 is the concentration at $x = 0$ at time t. Therefore plots of $\ln(C/C_0)$ against x^2/t should be linear with slope $= -1/(4D)$. There are two limiting cases: either (i) there is no significant transfer between the extra- and intra-particle spaces on the timescale of diffusion along the column, in which case $C = \theta_e' L_e + \rho S_e = (\theta_e' + \rho\beta_e)L_e$, and

$$D = D_l \theta_e' f_e / (\theta_e' + \rho\beta_e), \qquad (27)$$

or (ii) extra- to intra-particle equilibration is effectively instantaneous, in which case $C = \theta_e' L_e + \theta_i' L_i + \rho S_e + \rho S_i =$

© 2009 The Authors

$(\theta_e' + \theta_i' + \rho\beta)L_e$, and

$$D = D_l\theta_e' f_e/(\theta_e' + \theta_i' + \rho\beta). \quad (28)$$

Between these limits the relationships will be curved.

Figure 2 gives plots of $\ln(C/C_0)$ versus x^2/t for the single porosity model with the two limiting cases, and for the dual porosity model with different rates of intra-particle diffusion as represented by different values of the intra-particle diffusion impedance factor, f_i. Three types of solute reaction are compared: (i) no sorption, (ii) instantaneous sorption and (c) instantaneous sorption plus continuing slow sorption.

The relationships for no sorption (Figure 2a) are approximately linear, and the line for the single porosity model with instantaneous intra-particle equilibration is approached. There is some tendency to curvature near the $x = 0$ boundary, particularly for smaller f_i values. This is because, if diffusion out of the particles is slow, solute will tend to accumulate within particles as the peak of the solute pulse passes, and this effect increases as distance behind the peak increases, i.e. towards $x = 0$. The relationships for sorbed solutes (Figure 2b and c) are also approximately linear at large f_i values (for fast intra-particle diffusion), but they are increasingly curved as f_i decreases. For a given value of f_i, as sorption increases diffusion into and out of the particles is increasingly rate-limiting. The effect of the additional slow sorption reaction is small on the timescale of the runs shown (5×10^6 s, = 58 days).

The approximately linear relationships with large values of f_i are consistent with the experimental results listed above for the non-adsorbed Cl^- ion and for exchangeable Na^+, Ca^{2+}, Rb^+ and Cs^+ cations. The curved relationships with $f_i \leq 0.001$ are consistent with the experimental results for strongly-sorbed phosphate anions. These results imply that f_i, as we have defined it, varies between solutes. The linear experimental relationships for the exchangeable cations imply large f_i values, in spite of substantial sorption. Comparison of measured diffusion coefficients for these cations with those expected for diffusion in the liquid phase alone (references above) indicates that they retain significant mobility in the sorbed state on soil surfaces, contributing between 27 and 97% to the overall diffusion coefficient depending on the cation. If equilibration between the soil solution and solid is very rapid, as it will be for freely exchangeable cations, the solution and solid diffusion pathways partly act in series and so it is not possible to separate them. Further, being positively charged, cations are not excluded from very narrow pores by electrostatic repulsion. Hence equilibration between intra- and extra-particle pores is likely to be faster for these cations than for phosphate anions, which are essentially immobile on soil surfaces and are excluded from narrow pores to a greater extent. The effective value of f_i is therefore larger than for phosphate anions. We anticipate that specifically adsorbed cations, such as most transition metals, will also lack surface mobility and behave more like strongly sorbed phosphate.

The additional slow sorption reaction had little effect on overall diffusion through the soil. For the standard parameter values, the concentration of slowly reacting sites is three times that of rapid sites. Hence the model predicts that only a small proportion of the sorption sites that potentially participate in the diffusion process actually did so. This partly reflects the nature of the pulsed boundary condition and the fact that at a particular distance along the soil column, the sorption sites are first exposed to an increasing solute concentration and then to a decreasing one as the solute peak passes. The reaction times at individual sites are correspondingly curtailed. This is not the case for a constant source or sink of solute at the surface, as in the next two applications.

Constant concentration at soil surface. Figure 3 shows the predicted concentration-distance profiles in a soil column with a constant concentration C_0 at the surface $x = 0$ and zero initial concentration in the rest of the soil. For these conditions and instantaneous local equilibration, the single porosity model is (after Crank, 1975, Equation 3.13)

$$\frac{C}{C_0} = 1 - \text{erf}\frac{x}{2\sqrt{Dt}}, \quad (29)$$

where erf z is the error function. The profiles for rapid ($f_i = 10^{-2}$) and slow ($f_i = 10^{-3}$) access to intra-particle sites

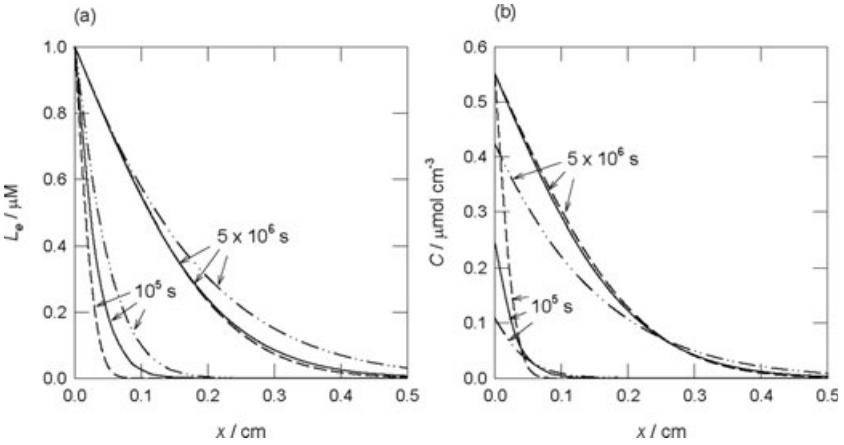

Figure 3 The effect of maintaining a constant concentration of a solute in solution at the surface of a soil column from which it was initially absent: (a) the concentration in the extra-particle liquid, (b) the total concentration in the soil. Solid lines: dual porosity model with rapid intra-particle diffusion ($f_i = 10^{-2}$). Dash-dot-dot lines: dual porosity model with slow intra-particle diffusion ($f_i = 10^{-3}$). Dashed lines: single porosity model with instantaneous equilibration with the intra-particle space. Sorption is instantaneous with no slow reactions.

© 2009 The Authors

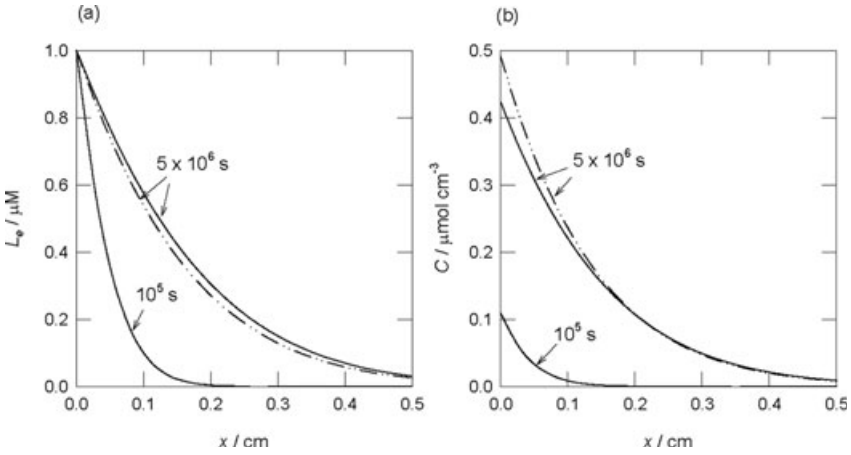

Figure 4 As Figure 3 with $f_i = 10^{-3}$ except: solid lines, with no slow reaction ($k_{F2} = 0$); dash-dot-dot lines, with slow reaction ($k_{F2} = 10^{-4}$ s^{-1}).

in the dual porosity model are compared with the profiles given by Equation (29) with D given by Equation (28) (instantaneous extra- to intra-particle equilibration).

Figure 3 shows that the spread of solution concentration is greater when there is slow access to the particles than with instantaneous access. However, the total amount of solute entering the soil, given by the area under the curve, is smaller because less accumulates within the particles. With slow access ($f_i = 0.001$), the concentration at $x = 0$ at $t = 10^5$ s is only a fifth of that for instantaneous intra-particle equilibration. The effect is smaller at longer times. Interestingly, the curves of total concentration cross over. Because the spread of solution concentration is greater at smaller f_i, the total concentration is greater far from the source. Nearer the source, total concentrations are larger at larger f_i because solute accumulates in the particles. The cross-over distance increases with time. Nye & Staunton (1994) obtained similar results with their model.

Figure 4 shows the effect of the rate constant for 'slow' sorption with the other parameters as standard. It shows that k_{F2} has little effect on the profiles in solution or the whole soil for values up to 10^{-4} s^{-1} and run times of several weeks. This is equivalent to a half-time of $t_{1/2} = \ln 2/k_{F2} = 6.93 \times 10^3$ s $\equiv$ 1.9 h, which is far faster than the very slow processes leading to equilibrium in well-mixed systems (Sposito, 2008). This shows that these slowly- reacting sites, which may dominate the long-term sorption equilibrium, are scarcely involved in the diffusion process. This implies that it is not necessary to allow for the slow reactions in modelling diffusion except at very long times. By contrast, Figure 3 shows that the rate limitation through diffusive penetration of the particles is clearly important both in terms of the spread of solute through the soil solution and the total amount sorbed.

Zero concentration at soil surface. Figure 5 shows the effect of maintaining a zero inter-particle solution concentration at the surface of a soil column containing a strongly-sorbed solute. This boundary condition is equivalent to a strong absorbent at the surface, such as a rapidly absorbing root mat. If the initial concentration throughout the soil is C_i, and local equilibration is instantaneous, then the single porosity model is (after Crank, 1975, Equation 3.13):

$$\frac{C}{C_i} = \mathrm{erf}\frac{x}{2\sqrt{Dt}}. \qquad (30)$$

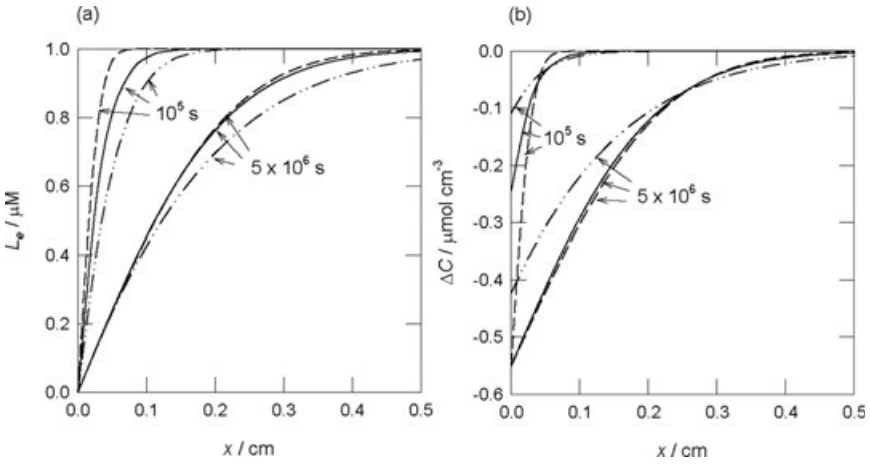

Figure 5 The effect of maintaining zero concentration of a solute in solution at the surface of a soil column from which it was initially uniformly distributed: (a) the concentration in the extra-particle liquid and (b) the change in total concentration in the soil. Solid lines, dual porosity model with rapid intra-particle diffusion ($f_i = 10^{-2}$); dash-dot-dot lines, dual porosity model with slow intra-particle diffusion ($f_i = 10^{-3}$); dashed lines, single porosity model with instantaneous equilibration with the intra-particle space. Sorption is instantaneous with no slow reactions.

© 2009 The Authors

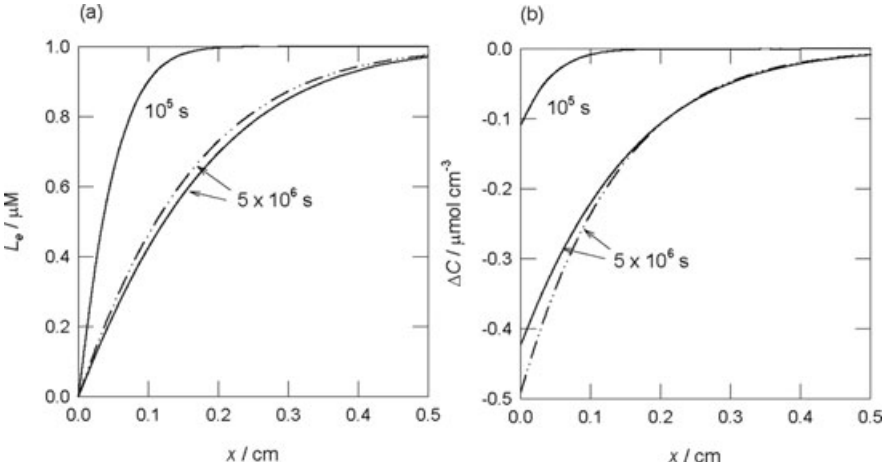

Figure 6 As in Figure 5 with $f_i = 10^{-3}$ except: solid lines, with no slow reaction ($k_{F2} = 0$); dash-dot-dot lines, with slow reaction ($k_{F2} = 10^{-4}$ s^{-1}).

As in Figure 3, the profiles calculated with the single and dual porosity models are compared in Figure 5.

The figure shows that solute depletion near the surface is strongly affected by the rate of intra-particle diffusion. If it is slow then the total solute released to the sink at $x = 0$ is decreased. With $f_i = 0.001$, the solute depletion at $x = 0$ at $t = 10^5$ s is only a fifth of that for instantaneous intra-particle equilibration. By contrast, Figure 6 shows the effect of the slow sorption reaction, as indicated by $k_{F2} = 10^{-4}$ s, is small, and slow sorption sites contribute little to the diffusion process, although, with the model parameter values used, they are three times more concentrated than the rapidly reacting sites. Hence, as for the results for adsorption, slow reaction has little net effect.

For a porosity of 0.1 (as for the intra-particle space in the model runs), the equivalent pore diameters in a medium textured soil are in the range 10–100 µm. For comparison, cereal roots can penetrate pores ≥100 µm in diameter, root hairs 5–20 µm in diameter and fungal hyphae 2–10 µm in diameter (Kilham, 1994). Given the slow rates of diffusion of strongly-sorbed solutes from pores of this diameter shown by the model, it is clear why very fine roots and fungal hyphae are crucial for plants to absorb such solutes.

Conclusions

1. Comparison of the single and dual porosity models shows that failure to allow correctly for slow access to sorption sites can lead to seriously erroneous predictions of diffusion through soil.
2. Slow access has the effect of decreasing the net rate of sorption of solute into soil from a source or of desorption from soil to a sink.
3. As a result, the diffusion coefficients of strongly-sorbed solutes measured at the macro-scale will be time dependent and will depend on the method of measurement.
4. For diffusion times up to several weeks, diffusion is dominated by rapidly equilibrating sorption sites; slowly-equilibrating sites, which may account for the majority of the final equilibrium sorption, are only important at very long times.
5. In principle, the unimportance of slow reactions simplifies modelling because, if slow access is correctly allowed for, sorption can be described with equilibrium relations based on understanding of speciation and rapid (<1 hour) sorption-desorption reactions. The problem then is to correctly describe diffusion limitations at the appropriate scale.
6. These conclusions broadly agree with those of Nye & Staunton (1994) for their less physically-realistic model.

Acknowledgements

This research was funded by BBSRC (Grant Ref. BB/C518014). TR is funded by a Royal Society University Research Fellowship. We thank Siobhan Staunton for commenting on the manuscript. We dedicate this paper to the late Peter Nye FRS, pioneer of soil diffusion studies.

References

Barrow, N.J. 2008. The description of sorption curves. *European Journal of Soil Science*, **59**, 900–910.

Bender, C.M. & Orszag, S.A. 1999. *Advanced Mathematical Methods for Scientists and Engineers. Asymptotic Methods and Perturbation Theory*. Springer-Verlag, New York.

Bourgeat, A., Luckhaus, S. & Mikelić, A. 1996. Convergence of the homogenization process for a double-porosity model of immiscible two-phase flow. *SIAM Journal on Mathematical Analysis*, **27**, 1520–1543.

Crank, J. 1975. *The Mathematics of Diffusion*. Oxford University Press, Oxford.

Ernstberger, H., Davison, W., Zhang, H., Tye, A. & Young, S. 2002. Measurement and dynamic modeling of trace metal mobilization in soils using DGT and DIFS. *Environmental Science & Technology*, **36**, 349–354.

Hornung, U. 1997. *Homogenization and Porous Media*. Springer-Verlag, Berlin.

© 2009 The Authors

Kevorkian, J. & Cole, J.D. 1996. *Multiple Scale and Singular Perturbation Methods*. Springer-Verlag, New York.

Kilham, K. 1994. *Soil Ecology*. Cambridge University Press, Cambridge.

Kirk, G.J.D., Solivas, J.L. & Alberto, M.A. 2003. The effects of redox conditions on solute diffusion in soil. *European Journal of Soil Science*, **54**, 617–624.

Nye, P.H. & Staunton, S. 1994. The self-diffusion of strongly adsorbed anions in soil: two-path model to simulate restricted access to exchange sites. *European Journal of Soil Science*, **45**, 145–152.

Pavliotis, G.A. & Stuart, A.M. 2008. *Multiscale Methods: Averaging and Homogenization*. Springer, New York.

Pinner, A. & Nye, P.H. 1982. A pulse method for studying effects of dead-end pores, slow equilibration and soil structure on diffusion of solutes in soil. *Journal of Soil Science*, **33**, 25–35.

So, H.B. & Nye, P.H. 1989. The effect of bulk density, water content and soil type on the diffusion of chloride in soil. *Journal of Soil Science*, **40**, 743–749.

Sposito, G. 2008. *The Chemistry of Soils*. Oxford University Press, Oxford.

Staunton, S. & Nye, P.H. 1989. Three approaches to the simulation of the self-diffusion and non-instantaneous isotopic exchange of phosphate in soil. *Journal of Soil Science*, **40**, 761–771.

Tinker, P.B. & Nye, P.H. 2000. *Solute Movement in the Rhizosphere*. Oxford University Press, Oxford.

Appendix: homogenization and derivation of macro-scale models using multiple scale asymptotic expansion

By re-scaling Equations (1a)–(5a) using $\mathbf{x} = \varepsilon\mathbf{y}$ we obtain the following model for a domain of unit length:

$$\frac{\partial L_e}{\partial t} = \nabla_x^2 L_e, \quad \text{in } \Omega^\varepsilon \tag{A1}$$

$$\frac{\partial(\theta_i L_i)}{\partial t} = \varepsilon^2 \hat{D}\nabla_x^2 L_i - \frac{\partial S_{i1}}{\partial t} - \frac{\partial S_{i2}}{\partial t}, \quad \text{in } \Omega_s^\varepsilon \tag{A2}$$

$$\nabla_x L_e \cdot \nu = \varepsilon^2 \hat{D}\nabla_x L_i \cdot \nu - \varepsilon\frac{\partial S_{e1}}{\partial t} - \varepsilon\frac{\partial S_{e2}}{\partial t}, \quad \text{on } \Gamma^\varepsilon \tag{A3}$$

$$L_e = L_i, \quad \text{on } \Gamma^\varepsilon \tag{A4}$$

$$\nabla_x L_e \cdot \nu = 0, \quad \text{on } \Gamma_g^\varepsilon \tag{A5}$$

where $\hat{D} = D_i/(D_l\varepsilon^2)$ and $\Omega^\varepsilon, \Omega_s^\varepsilon, \Gamma^\varepsilon$ and Γ_g^ε are the domains of the inter-particle space, the intra-particle space, the surfaces of all soil particles and the surfaces of all gas spaces, respectively. Equations (A1)–(A5) are defined in the complicated space domain Ω^ε consisting of many individual soil particles. For the final model we need equations for average concentrations defined in a simpler domain. We obtain these using homogenization techniques as follows. We give the equations for the model used in the main paper, which depends on the ratio of the diffusion coefficients in the intra- and inter-particle spaces (D_i/D_l) being of order ε^2. We also give the equations forD_i/D_l larger and smaller than this.

Equations for $D_i/D_l \approx \varepsilon^2$

To derive the macroscopic equations we use the following asymptotic expansions with respect to ε:

$$\begin{aligned} L_e &= L_e^0(x,y) + \varepsilon L_e^1(x,y) + \varepsilon^2 L_e^2(x,y) + \dots \\ L_i &= L_i^0(x,y) + \varepsilon L_i^1(x,y) + \varepsilon^2 L_i^2(x,y) + \dots \\ S_{en} &= S_{en}^0(x,y) + \varepsilon S_{en}^1(x,y) + \varepsilon^2 S_{en}^2(x,y) + \dots \\ S_{in} &= S_{in}^0(x,y) + \varepsilon S_{in}^1(x,y) + \varepsilon^2 S_{in}^2(x,y) + \dots \end{aligned} \tag{A6}$$

where $n = 1$ or 2 for the fast and slow reactions. The concentration variables in (A6) are periodic with respect to $\mathbf{y} = \mathbf{x}/\varepsilon$. In the multiple space scale, we have from the chain rule $\nabla = \nabla_x + 1/\varepsilon\nabla_y$. We combine Equations (A6) with Equations (A1)–(A5) and then compare the coefficients of the resulting equations for different powers of ε ($O(\varepsilon^k)$ where $k = 0, 1, 2$ etc) to obtain the sequence of problems at each power of ε. The variable $L_e^0(t,x)$ is a solution to the problem that comes from $O(\varepsilon^0)$ after solving the problems at $O(\varepsilon^{-2})$ and $O(\varepsilon^{-1})$ and averaging over the single particle scale problem, i.e. $L_e^0(t,x)$ solves

$$\begin{aligned} \theta_e'\frac{\partial L_e^0}{\partial t} &= \nabla_x\cdot(A_{\text{hom}}\nabla_x L_e^0) + \frac{1}{|Z|}\int_\Gamma \hat{D}\nabla_y L_i^0\cdot\nu d\gamma \\ &\quad - \frac{1}{|Z|}\int_\Gamma\left(\frac{\partial S_{e1}^0}{\partial t} + \frac{\partial S_{e2}^0}{\partial t}\right)d\gamma \end{aligned} \tag{A7}$$

where A_{hom} is a matrix for the effective macroscopic diffusion, with off-diagonal elements $a(i,j)$ because of the microstructure. This is given by:

$$A_{\text{hom}} = \theta_e'\delta_{ij} + \frac{1}{|Z|}\int_{Y_1}\frac{\partial w_j}{\partial y_i}dy, \tag{A8}$$

where δ_{ij} is Kroenecker's delta (= 1 if $i = j$, 0 if $i \neq j$) and w_j is defined by:

$$\begin{aligned} \nabla_y^2\, w_j &= 0 \quad \text{in } Y_1 \\ \nabla_y w_j\cdot\nu &= -e_j\cdot\nu \quad \text{on } \Gamma \\ \nabla_y w_j\cdot\nu &= -e_j\cdot\nu, \quad \text{on } \Gamma_1 \end{aligned}$$

where e_j is the unit vector for the jth coordinate axis: $e_1 = (1,0,0)$, $e_2 = (0,1,0)$, $e_3 = (0,0,1)$ and w_j is periodic in Y_1 such that $\int_{Y_1} w_j dy = 0$. Similarly $L_i^0(t,x,y)$ solves:

$$\frac{\partial L_i^0}{\partial t} = \hat{D}\nabla_y^2 L_i^0 - \frac{\partial S_{i1}^0}{\partial t} - \frac{\partial S_{i2}^0}{\partial t}, \tag{A9}$$

with $L_i^0 = L_e^0$ on $\Gamma\times\Omega$. The solution of the integral term in Equation (A8) for the geometry specified in Figure 1, obtained

© 2009 The Authors
Journal compilation © 2009 British Society of Soil Science,

with Comsol Multiphysics, is:

$$\int_{Y_1} \frac{\partial w_j}{\partial y_i} dy = -0.102\delta_{ij}.$$

Thus, since $\theta_e' = 0.274$ (Parameter values), $A_{\text{hom}}^{ij} = 0.172\delta_{ij}$. Because of the geometry, that is a spherical particle, there are no off-diagonal elements in our diffusion matrix and so we have standard impeded diffusion with $A_{\text{hom}} = \theta_e' f_e = 0.172$.

Equations for $D_i/D_l \approx \varepsilon$

In Equations (A1)–(A5), ε^2 is replaced by ε and $\hat{D} = D_i/(D_l\varepsilon)$ is of order one. Thus, in contrast to the case of $D_i/D_l \approx \varepsilon^2$ where the single particle term appeared at the $O(\varepsilon^0)$ problem, the single particle dynamics now appear in the $O(\varepsilon^{-1})$ problem. Hence, the concentration within the particle L_i^0 is undisturbed and depends only on the macroscopic variable **x**. Thus, as in the previous case, the equation for average macroscopic concentrations comes from the $O(\varepsilon^0)$ problem and $L = L_e(x) = L_i(x)$ is given by:

$$\left(\theta_e' + \frac{|Y|\theta_i}{|Z|}\right)\frac{\partial L}{\partial t} = \nabla_x\cdot(A_{\text{hom}}\nabla_x L) - \frac{1}{|Z|}\int_\Gamma \left(\frac{\partial S_{e1}^0}{\partial t} + \frac{\partial S_{e2}^0}{\partial t}\right)d\gamma - \frac{1}{|Z|}\int_Y \left(\frac{\partial S_{i1}^0}{\partial t} + \frac{\partial S_{i2}^0}{\partial t}\right)dy, \tag{A10}$$

where A_{hom} is defined in the same way as for $D_i/D_l \approx \varepsilon^2$. Hence when$D_i/D_l \approx \varepsilon$, we find that only the rate of reaction inside the particle is important on the macroscopic scale because the diffusion of the solute inside the particle is effectively instantaneous.

Equations for $D_i/D_l \approx \varepsilon^3$

In Equations (A1)–(A5), ε^2 is replaced by ε^3 and $\hat{D} = D_i/(D_l\varepsilon^3)$ is of order one. Following the same procedures as for $D_i/D_l \approx \varepsilon$ we obtain:

$$\begin{aligned}\theta_e'\frac{\partial L_e^0}{\partial t} &= \nabla_x\cdot(A_{\text{hom}}\nabla_x L_e^0) - \frac{1}{|Z|}\int_\Gamma \left(\frac{\partial S_{e1}^0}{\partial t} + \frac{\partial S_{e2}^0}{\partial t}\right)d\gamma \quad \text{on } \Gamma\times\Omega \\ \frac{\partial L_i^0}{\partial t} &= -\frac{\partial S_{i1}^0}{\partial t} - \frac{\partial S_{i2}^0}{\partial t}. \quad \text{in } \mathrm{Y}\times\Omega\end{aligned} \tag{A11}$$

The flux into the particle is of order ε^3, which is small because $\nabla L_i^0 \times$ particle volume $= (\nabla_x + 1/\varepsilon\nabla_y)\cdot C\cdot\varepsilon^3 \approx O(\varepsilon^2)$. Thus the diffusion into and inside the particle is not apparent on the macroscopic scale and the equations for the concentrations inside the particle are not coupled with the macroscopic equations in the inter-particle space.

© 2009 The Authors